IEEE Photonics Journal
An IEEE Photonics Society Publication

Open Access

Circular Dichroism in Planar Achiral Plasmonic L-Shaped Nanostructure Arrays

Volume 9, Number 2, April 2017

Yongyuan Zhang
Li Wang
Zhongyue Zhang

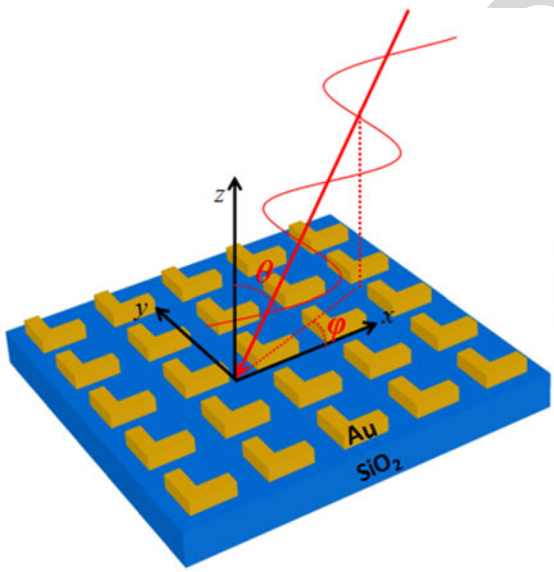

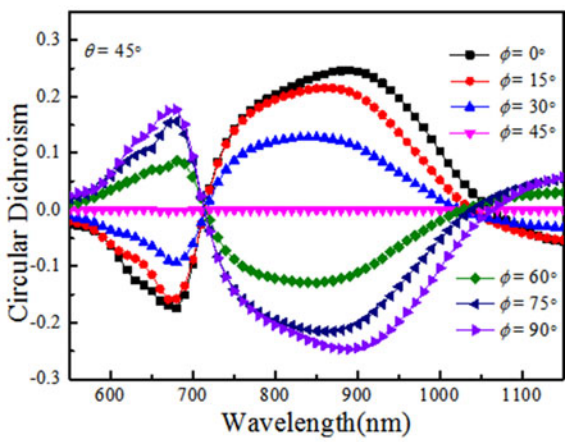

DOI: 10.1109/JPHOT.2017.2670783
1943-0655 © 2017 IEEE

IEEE photonics SOCIETY

IEEE

Circular Dichroism in Planar Achiral Plasmonic L-Shaped Nanostructure Arrays

Yongyuan Zhang,[1,2] Li Wang,[1] and Zhongyue Zhang[1]

[1]School of Physics and Information Technology, Shaanxi Normal University, Xi'an 710062, China
[2]School of Science, Xi'an University of Science and Technology, Xi'an 710054, China

DOI:10.1109/JPHOT.2017.2670783

Manuscript received December 21, 2016; accepted February 14, 2017. This work was supported in part by the National Natural Foundation of China under Grant 61575117, in part by the Fundamental Research Funds for the Central Universities under Grant GK201601008, and in part by the Fostering Fund of Xian university of Science and Technology under Grant 2010045. Corresponding author: Z. Zhang (e-mail: zyzhang@snnu.edu.cn).

Abstract: Circular dichroism (CD) can be initially observed in intrinsic chiral structures. It was discovered that CD can also be observed in achiral structures with an oblique incident light beam. In this paper, a metal planar achiral L-shaped nanostructure arrays was proposed, and its CD was investigated using the finite element method. The CD phenomenon is due to extrinsic chirality resulting from the achiral structures with an oblique incident electromagnetic wave. Results show that the L-shaped nanostructure arrays can achieve strong and broad bandwidth CD. In addition, the sign of CD can be reversed through changing azimuthal rotation angle of incident light, and the strength of CD depends strongly on light incident direction.

Index Terms: Circular dichroism, oblique incidence, surface plasmon.

1. Introduction

Chiral structures cannot be superimposed with their mirror images [1]–[3]. Chiral structures and their images are called chiral enantiomers. Chirality is a universal feature of nature and is closely related to the phenomenon of life. Chirality played a key role in the biochemistry and evolution of life [4]. Many of the basic composition of life, such as proteins, amino acids and ribonucleic acid are chiral. Different optical response of chiral structures to left circularly polarized (LCP) and right-handed circularly polarized light (RCP), known as circular dichroism (CD).

In recent years, the CD effects of chiral plasmonic nanostructures were studied extensively in theoretical and experimental [5]–[14]. Compared to most natural chiral molecules, artificial plasmonic nanostructures can exhibit very strong chiroptical effects due to a much larger dipole moment of the localized surface plasmon (LSP) resonance and accordingly a stronger interaction with external light field. A number of three-dimensional (3-D) chiral nanostructures have been proposed, such as metal helix structures [15]–[17] and layer by layer chiral plasmonic nanostructures [18]–[30]. Compared to the 3-D chiral nanostructures, the planar achiral nanostructures are easier to fabricate. When planar achiral nanostructures, such as elliptical nanoholes [31], [32] and asymmetric split

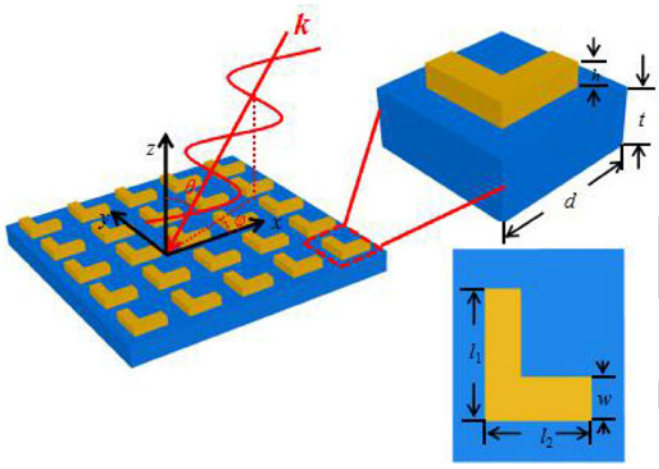

Fig. 1. Schematic diagram of L-shaped nanostructure array and its unit cell.

ring structures [33]–[36], are subjected to obliquely incident light, strong CD appear, which was termed as "extrinsic chiral" [37].

However, the CD effects of the most plasmonic nanostructures have been restricted to narrow frequency ranges, which is a major drawback for many potential applications. The research of broadband CD effect to realize the broadband circularly polarized light excitation and collection, has wider significance. Broadband infrared circular polarizers based on gold helical metamaterials [16] have been recently demonstrated; however, realizing these structures in the visible is hindered by their fabrication becomes challenging as their geometrical dimensions get smaller.

In this paper, we proposed periodic L-shaped nanostructure arrays above a dielectric substrate and studied their CD effect. The CD effect is tunable; its sign and magnitude are controlled by light incident direction. Importantly, this type of tunable CD occurs in simple planar structure designs that are ideally suited for well-established planar manufacturing technologies.

2. Structure and Computational Method

The schematic geometry of proposed L-shaped gold nanostructure arrays is shown in Fig. 1. The L-shaped nanostructure arrays rests on top of a substrate with refractive indices 1.444 and thickness $t = 200$ nm. The period of the unit cell is $d = 250$ nm. The dimensions of the L-shaped nanostructure are shown in the right panel of Fig. 1. The thickness and width are as $t = 40$ nm and $w = 50$ nm, respectively. The arm lengths are denoted as l_1 and l_2, respectively. The refractive index of gold is obtained from [38]. The angle between the incident wave vector **k** and the plane normal is denoted as the tilted angle θ. The azimuthal rotation angle of the incident wave vector is ϕ.

The transmission coefficients and surface charge distributions of the L-shaped nanostructure arrays are investigated using the RF module of the finite element-based software COMSOL Multiphysics 4.3. The transmission coefficient is defined as the rate of output power P_{out} to input power P_{in}, namely, $T = P_{out}/P_{in}$. We use subscripts $+$ and $-$ denote RCP and LCP light correspondingly. T_{++} (T_{--}) represents the transmittance of RCP (LCP) light. Then, CD is defined as CD $= T_{++} - T_{--}$.

3. Results and Discussion

Fig. 2(a)–(d) show the transmission spectra for LCP and RCP light incident on the L-shaped nanostructure arrays at θ from 0° to 60° in the case of $\phi = 0°$. Two evident resonant modes, namely, λ_I and λ_{II} around 990 and 700 nm are observed in the transmission spectra from 550 to 1150 nm at $\theta = 0°$ as shown in Fig. 2(a). These modes are labeled as I and II, respectively.

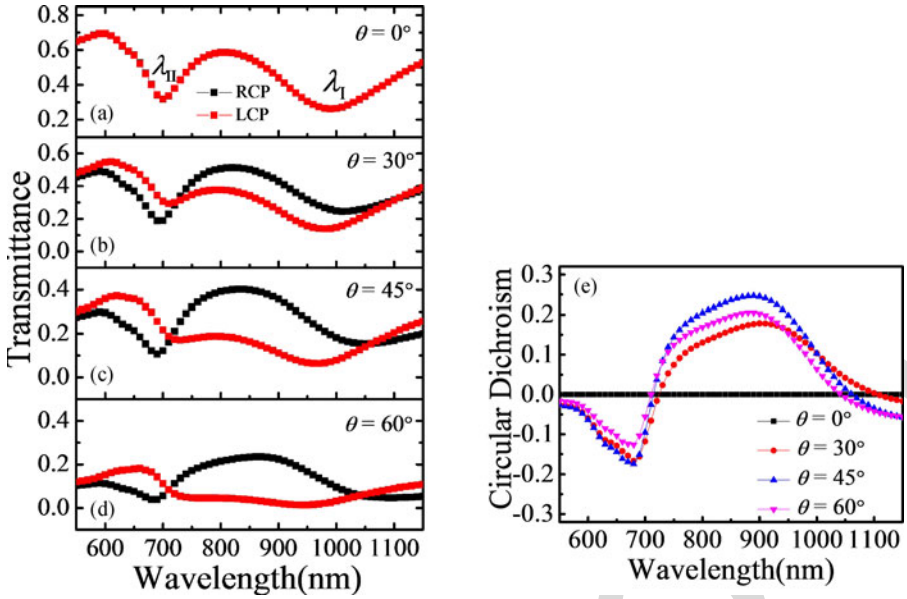

Fig. 2. (a)–(d) Transmission spectra of LCP and RCP light at $\phi = 0$○ (a), $\theta = 30^\circ$ (b), $\theta = 45^\circ$ (c), and $\theta = 60^\circ$ (d). (e) CD spectra at $\theta = 0^\circ$, $\theta = 30^\circ$, $\theta = 45^\circ$, and $\theta = 60^\circ$.

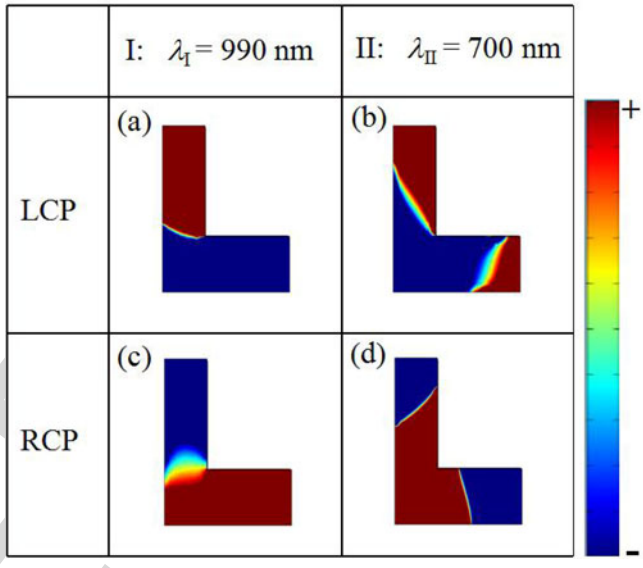

Fig. 3. Surface charge distributions of Mode I (a) and mode II (b) under LCP incidence, as well as mode I (c) and mode II (d) under RCP incidence.

Fig. 2(e) is the CD spectra of L-shaped nanostructure arrays with different θ. Note there is no CD effect at $\theta = 0^\circ$. The L-shaped nanostructure arrays have strong and broad bandwidth CD effect with oblique incidence between 750 and 950 nm due to the two resonant modes get closer under LCP illumination but get wider under RCP illumination. Thus, the L-shaped nanostructure arrays operate as a broadband circular polarizer in this region. When θ increases from 0° to 60°, the absolute value of the CD increases at first and then decreases, leading to a moderate θ of 45°.

To depict this phenomenon in Fig. 2, we calculated the surface charge distributions of the L-shaped nanostructure arrays at resonant modes. Fig. 3 shows the surface charge distributions

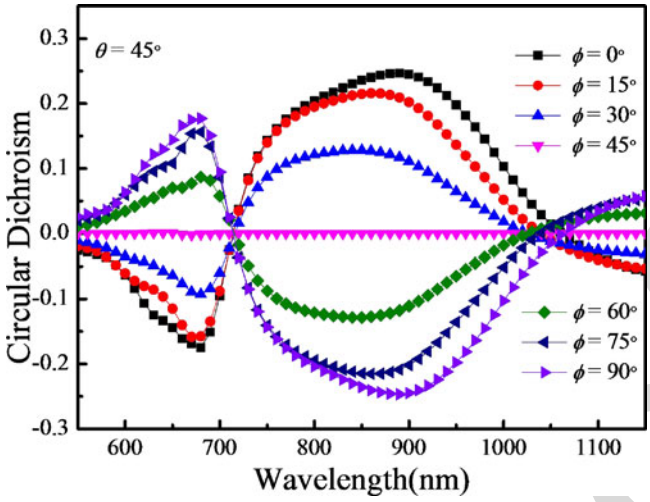

Fig. 4. CD spectra of the L-shaped nanostructure arrays at $\theta = 45^\circ$ with different ϕ.

of the L-shaped nanostructure arrays under circularly polarized light illumination with $\phi = 0^\circ$ and $\theta = 0^\circ$ at the resonant wavelengths. The surface charge distributions of the L-shaped nanostructure arrays under LCP illumination at the two resonant wavelengths as shown in Fig. 3(a) and (b). Fig. 3(c) and (d) show the surface charge distributions under RCP illumination at the two resonant wavelengths. At $\lambda_{\mathrm{I}} = 990$ nm, the distribution of positive and negative surface charge corresponds to the two arms of the L-shaped nanostructure [see Fig. 3(a) and (c)], which form the effective dipole electron oscillation. At $\lambda_{\mathrm{II}} = 700$ nm, the same polarity surface charge separated by the opposite charge distribute in both ends of the two arms [see Fig. 3(b) and (d)], which form the effective quadruple electron oscillation. Thus the formation of mode I and II are due to LSP effective dipole electron oscillation and quadruple electron oscillation, respectively.

The CD spectra of the L-shaped nanostructure arrays taken at several ϕ angles in the case of $\theta = 45^\circ$ as shown in Fig. 4. The CD signal is significant only when the array is subjected to obliquely incident light and without a symmetry axis in the plane of incidence, that is, $\theta \neq 0^\circ$, $\phi \neq 45^\circ$. The CD spectra show a monotonic decrease in absolute value followed by an inversion of the sign and subsequent monotonic increase in the absolute CD value. The L-shaped nanostructure changes to its enantiomer when the ϕ changed to symmetrical about 45°. Thus, we can change the handedness of L-shaped nanostructure by tuning ϕ rather than by rebuilding the structure.

The mechanism of external chirality can be thought relating to optical activity of a chiral molecule, where the effect comes from interaction of the electric and magnetic responses. Similar to a chiral molecule, the CD effect of a plasmonic structure is estimated by the general equation [39]

$$\mathrm{CD} \propto \mathrm{Im}[\vec{p} \cdot \vec{m}] \tag{1}$$

where $\vec{p}$ and $\vec{m}$ are the electric and magnetic dipole moments of the plasmonic structure. Here, in the L-shaped nanostructure arrays, in the case of RCP light incident at $\phi = 30^\circ$ and $\theta = 45^\circ$, the excited surface current distributions induce corresponding electric and magnetic dipole moments, respectively, as shown in Fig. 5(a). The component of the electric dipole moments $\vec{p}$ respect to x axis and y axis marked as p_x and p_y, respectively, and $p_y = p \cdot \sin 45^\circ$, $p_x = p \cdot \cos 45^\circ$. When the light was at oblique incident, both moments $\vec{p}$ and $\vec{m}$ of the mode I have projections in the plane perpendicular to the light incident direction, marked as p'_x, p'_y *and* m', respectively [see Fig. 6(b)], and $m' = m \cdot \sin\theta$, $p'_x = p_x \cdot \cos\theta\cos\phi$, and $p'_y = p_y \cdot \cos\theta\sin\phi$. The superposition of p'_x and p'_y at the

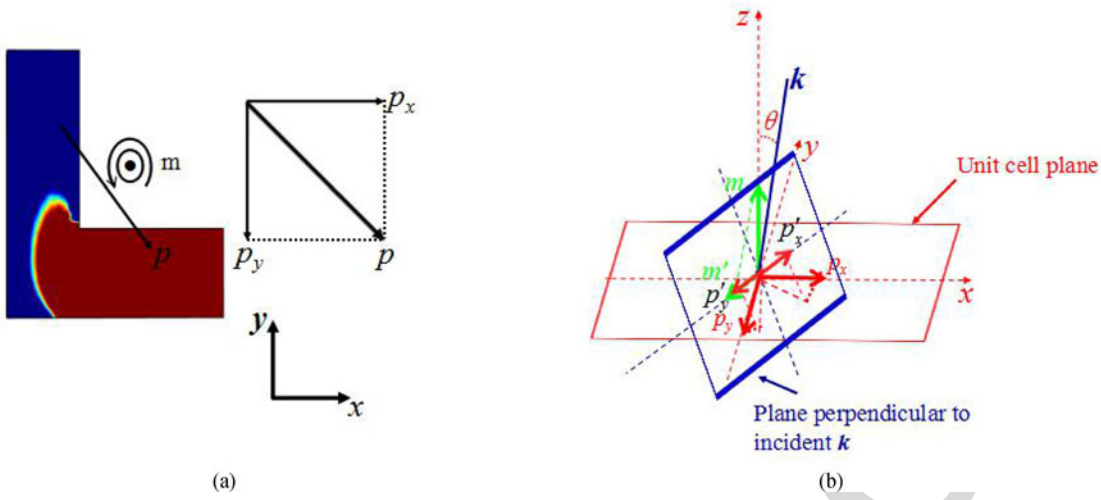

Fig. 5. (a) Surface charge distributions at mode I excited by RCP light and at $\phi = 30°$ and $\theta = 45°$. Induced equivalent electric dipole and magnetic dipole moments are marked as "*p*" and "*m*." (b) Schematic of CD generation mechanism at mode I. The projections of magnetic dipole moment *m*′ and the electric dipole moment p′ in the plane perpendicular to the incident light can reduce LCP light but increase RCP light, generating the CD.

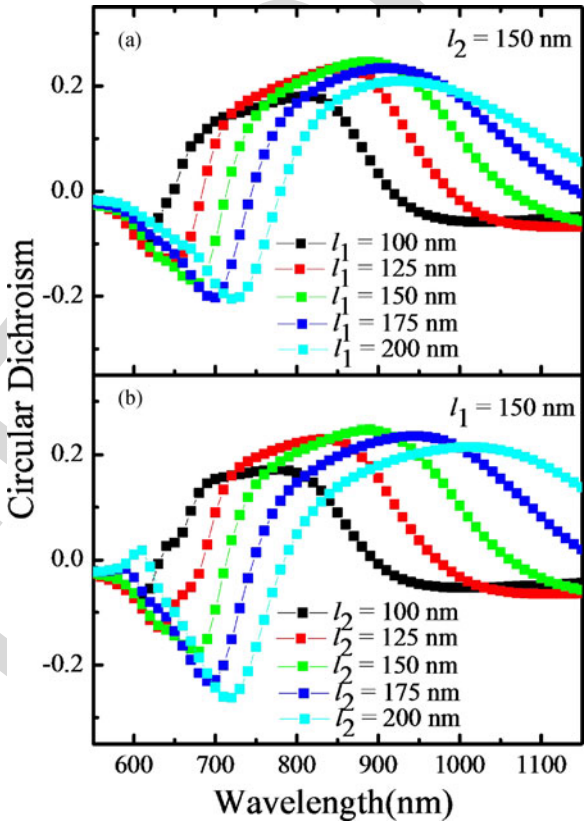

Fig. 6. CD spectra of the L-shaped nanostructure arrays at $\theta = 45°$ and $\phi = 0°$ with different arm lengths. (a) Different l_1. (b) Different l_2.

direction of m′ is defined as p'

$$p' = p'_y - p'_x = p_y \cdot \cos\theta \sin\phi - p_x \cdot \cos\theta \cos\phi$$
$$= \frac{\sqrt{2}}{2} p \cdot (\cos\theta \sin\phi - \cos\theta \cos\phi)$$
$$= p \cdot \cos\theta \cdot \sin(\phi - 45^\circ). \quad (2)$$

Thus

$$\mathrm{CD} \propto \mathrm{Im}[\vec{p} \cdot \vec{m}] \propto \mathrm{Im}[p \cdot m \cdot \sin 2\theta \cdot \sin(\phi - 45^\circ)]. \quad (3)$$

For fixed ϕ, maximum CD occurs at $\theta = 45^\circ$ and minimum CD occurs at $\theta = 0^\circ$, which is consistent with the results in Fig 2(e). For fixed θ, minimum CD occurs at $\phi = 45^\circ$ and maximum CD occurs at $\phi = 0^\circ$ and $\phi = 90^\circ$, which is consistent with the results in Fig. 4.

Fig. 6 shows the CD spectra for fixed angles $\theta = 45^\circ$ and $\phi = 0^\circ$ with different arm lengths as other parameters unchanged. Fig. 6(a) shows the CD spectra of the L-shaped nanostructure as l_1 increases from 100 nm to 200 nm with fixed $l_2 = 150$ nm. Fig. 6(b) shows the CD spectra of the L-shaped nanostructure as l_2 increases from 100 nm to 200 nm with fixed $l_1 = 150$ nm. With the increase of the lengths of two arms, both mode I and mode II red-shift, which leads to the red-shift of the broad CD band. The red-shift of mode I and mode II are due to the increasing the electron oscillation length as lengths of two arms increase.

4. Conclusion

A strong and broad bandwidth CD effect was observed in plasmonic L-shaped nanostructure arrays. The parallel components of the electric and magnetic dipole moments in the plane perpendicular to the incident light result in the CD effect. The two resonant modes get closer under one circularly polarized light illumination but get wider under the other circularly polarized light illumination with oblique incidence, thus realize the broad bandwidth CD effect. The ability to obtain the two "enantiomers" from the same arrays with the azimuthal rotation angle changed to symmetrical about the symmetry axis of the structure will eliminate various problems accompanying the fabrication of exact mirror image left- and right-intrinsically chiral structure. Moreover, the CD effect can be conveniently tuned due to the strength of CD depend strongly on tilt angle at the same azimuthal rotation angle. In addition, the broad CD band can be tuned by changing the geometrical parameters of the structure. Given the strong and broad bandwidth CD effect, the proposed structure is potential for building ultra-compact polarization components in integrated photonics and broadband circular polarizer.

References

[1] A. O. Govorov, Z. Y. Fan, P. Hernandez, J. M. Slocik, and R. R. Naik, "Theory of circular dichroism of nanomaterials comprising chiral molecules and nanocrystals: Plasmon enhancement, dipole interactions, and dielectric effects," *Nano Lett.*, vol. 10, no. 4, pp. 1374–1382, Feb. 2010.

[2] M. Schaferling, D. Dregely, M. Hentschel, and H. Giessen, "Tailoring enhanced optical chirality: Design principles for chiral plasmonic nanostructures," *Phys. Rev. X*, vol. 2, no. 3, 2012, Art. no. 031010.

[3] V. K. Valev, J. J. Baumberg, C. Sibilia, and T. Verbiest, "Chirality and chiroptical effects in plasmonic nanostructures: Fundamentals, recent Progress, and outlook," *Adv. Mater.*, vol. 25, no. 18, pp. 2517–2534, 2013.

[4] J. M. Slocik, A. O. Govorov, and R. R. Naik, "Plasmonic circular dichroism of peptide-functionalized gold nanoparticles," *Nano Lett.*, vol. 11, no. 2, pp. 701–705, Jan. 2011.

[5] B. M. Maoz *et al.*, "Amplification of chiroptical activity of chiral biomolecules by surface plasmons," *Nano Lett.*, vol. 13, no. 3, pp. 1203–1209, Feb. 2013.

[6] M. Hentschel, L. Wu, M. Schaferling, P. Bai, E. P. Li, and H. Giessen, "Optical properties of chiral three-dimensional plasmonic oligomers at the onset of charge-transfer plasmons," *ACS Nano*, vol. 6, no. 11, pp. 10355–10365, Oct. 2012.

[7] Z. T. Li *et al.*, "Reversible plasmonic circular dichroism of Au nanorod and DNA assemblies," *J. Amer. Chem. Soc.*, vol. 134, pp. 3322–3325, Feb. 2012.

[8] F. Lu *et al.*, "Discrete nanocubes as plasmonic reporters of molecular chirality," *Nano Lett.*, vol. 13, no. 7, pp. 3145–3151, Jun. 2013.

[9] A. Sharma, T. Mori, H. C. Lee, M. Worden, E. Bidwell, and T. Hegmann, "Visualizing, and measuring gold nanoparticle chirality using helical pitch measurements in nematic liquid crystal phases," *ACS Nano*, vol. 8, no. 12, pp. 11966–11976, Nov. 2014.

[10] M. Hentschel, V. E. Ferry, and A. P. Alivisatos, "Optical rotation reversal in the optical response of chiral plasmonic nanosystems: The role of plasmon hybridization," *ACS Photon.*, vol. 2, pp. 1253–1259, Aug. 2015.

[11] S. M. Swasey, N. Karimova, C. M. Aikens, D. E. Schultz, A. J. Simon, and E. G. Gwinn, "Chiral electronic transitions in fluorescent silver clusters Stabilized by DNA," *ACS Nano*, vol. 8, no. 7, pp. 6883–6892, Jun. 2014.

[12] X. B. Shen *et al.*, "3D plasmonic chiral colloids," *Nanoscale*, vol. 6, no. 4, pp. 2077–2081, Jun. 2014.

[13] M. Kuwata-Gonokami *et al.*, "Condensed matter: Electronic properties, etc. Giant optical activity in quasi-two-dimensional planar nanostructures," *Phys. Rev. Lett.*, vol. 95, no. 22, 2005, Art. no. 227401.

[14] A. S. Schwanecke, V. A. Fedotov, V. V. Khardikov, S. L. Prosvirnin, Y. Chen, and N. I. Zheludev, "Nanostructured metal film with asymmetric optical transmission," *Nano Lett.*, vol. 8, no. 9, pp. 2940–2943, Aug. 2008.

[15] J. K. Gansel, M. Latzel, A. Frolich, J. Kaschke, M. Thiel, and M. Wegener, "Tapered gold-helix metamaterials as improved circular polarizers," *Appl. Phys. Lett.*, vol. 100, no. 10, Mar. 2012, Art. no. 101109.

[16] J. K. Gansel *et al.*, "Gold helix photonic metamaterial as broadband circular polarizer," *Science*, vol. 325, no. 5974, pp. 1513–1515, 2009.

[17] J. Kaschke, J. K. Gansel, and M. Wegener, "On metamaterial circular polarizers based on metal N-helices," *Opt. Exp.*, vol. 20, no. 23, pp. 26012–26120, May 2012.

[18] J. F. Zhou, J. F. Dong, B. N. Wang, T. Koschny, M. Kafesaki, and C. M. Soukoulis, "Negative refractive index due to chirality," *Phys. Rev. B*, vol. 79, no. 12, Mar. 2009, Art. no. 121104.

[19] Y. Zhao, M. A. Belkin, and A. Alù, "Twisted optical metamaterials for planarized ultrathin broadband circular polarizers," *Nat. Commun.*, vol. 3, May 2012, Art. no. 870.

[20] L. Wu *et al.*, "Electromagnetic manifestation of chirality in layer-by-layer chiral metamaterials," *Opt. Exp.*, vol. 21, no. 5, pp. 5239–5246, Mar. 2013.

[21] X. H. Yin, M. Schäferling, B. Metzger, and H. Giessen, "Interpreting chiral nanophotonic spectra: The plasmonic Born–Kuhn Model," *Nano Lett.*, vol. 13, no. 12, pp. 6238–6243, Nov. 2013.

[22] Y. H. Cui, L. Kang, S. F. Lan, S. Rodrigues, and W. S. Cai, "Giant chiral optical response from a twisted-arc metamaterial," *Nano. Lett.*, vol. 14, no. 2, pp. 1021–1025, Jan. 2014.

[23] M. Decker, R. Zhao, C. M. Soukoulis, S. Linden, and M. Wegener, "Twisted split-ring-resonator photonic metamaterial with huge optical activity," *Opt. Lett.*, vol. 35, no. 10, pp. 1593–1595, May 2010.

[24] Z. F. Li *et al.*, "Chiral metamaterials with negative refractive index based on four "U" split ring resonators," *Appl. Phys. Lett.*, vol. 97, no. 8, Aug. 2010, Art. no. 081901.

[25] X. Xiong *et al.*, "Construction of a chiral metamaterial with a U-shaped resonator assembly," *Phys. Rev. B*, vol. 81, no. 7, Feb. 2010, Art. no. 075119.

[26] J. F. Dong, J. F. Zhou, T. Koschny, and C. Soukoulis, "Bi-layer cross chiral structure with strong optical activity and negative refractive index," *Opt. Exp.*, vol. 17, no. 16, pp. 14172–14179, Aug. 2009.

[27] M. Decker *et al.*, "Strong optical activity from twisted-cross photonic metamaterials," *Opt. Lett.*, vol. 34, no. 16, pp. 2501–2503, Aug. 2009.

[28] R. Zhao, L. Zhang, J. Zhou, Th. Koschny, and C. M. Soukoulis, "Conjugated gammadion chiral metamaterial with uniaxial optical activity and negative refractive index," *Phys. Rev. B*, vol. 83, no. 3, Jan. 2011, Art. no. 035105.

[29] T. Cao, L. Zhang, R. E. Simpson, C. W. Wei, and M. J. Cryan, "Strongly tunable circular dichroism in gammadion chiral phase-change metamaterials," *Opt. Exp.*, vol. 21, no. 23, pp. 27841–27851, Nov. 2013.

[30] Z. F. Li, K. B. Alici, E. Colak, and E. Ozbay, "Complementary chiral metamaterials with giant optical activity and negative refractive index," *Appl. Phys. Lett.*, vol. 98, no. 16, Apr. 2011, Art. no. 161907.

[31] T. Cao and M. J. Cryan, "Circular dichroism in planar nonchiral metamaterial made of elliptical nanoholes array," *J. Electromagn. Waves Appl.*, vol. 26, no. 10, pp. 1275–1282, Jul. 2012.

[32] T. Cao and M. J. Cryan, "Enhancement of circular dichroism by a planar non-chiral magnetic metamaterial," *J. Opt.*, vol. 14, no. 8, pp. 85101–85106, Jul. 2012.

[33] J. H. Shi, Z. Zhu, H. F. Ma, W. X. Jiang, and T. J. Cui, "Tunable symmetric and asymmetric resonances in an asymmetrical split-ring metamaterial," *J. Appl. Phys.*, vol. 112, no. 7, pp. 073522–073526, Oct. 2012.

[34] E. Plum, V. A. Fedotov, and N. I. Zheludev, "Extrinsic electromagnetic chirality in metamaterials," *J. Opt. A*, vol. 11, no. 7, May 2009, Art. no. 074009.

[35] R. Singh, E. Plum, W. L. Zhang, and N. I. Zheludev, "Highly tunable optical activity in planar achiral terahertz metamaterials," *Opt. Exp.*, vol. 18, no. 13, pp. 13425–13430, Jun. 2013.

[36] E. Plum, V. A. Fedotov, and N. I. Zheludev, "Optical activity in extrinsically chiral metamaterial," *Appl. Phys. Lett.*, vol. 93, no. 19, Nov. 2008, Art. no. 191911.

[37] E. Plum, X. X. Liu, V. A. Fedotov, Y. Chen, D. P. Tsai, and N. I. Zheludev, "Metamaterials: Optical activity without chirality," *Phys. Rev. Lett.*, vol. 102, no. 11, Mar. 2009, Art. no. 113902.

[38] P. B. Johnson and R. W. Christy, "Optical constants of the noble metals," *Phys. Rev. B*, vol. 6, no. 12, pp. 4370–4379, Jul. 1972.

[39] L. D. Barron, *Molecular Light Scattering and Optical Activity*, 2nd ed. Cambridge, U.K.: Cambridge Univ. Press, 2004.